Jay F. Storz Publications

Papers in the Biological Sciences

6-14-2013

Epistasis Among Adaptive Mutations in Deer Mouse Hemoglobin

Chandrasekhar Natarajan
University of Nebraska-Lincoln, chandrasekhar.natarajan@unl.edu

Noriko Inoguchi
University of Nebraska-Lincoln, ninoguchi2@unl.edu

Roy E. Weber
Aarhus University, Denmark, roy.weber@biology.au.dk

Angela Fago
Aarhus University, Denmark, angela.fago@biology.au.dk

Hideaki Moriyama
University of Nebraska-Lincoln, hmoriyama2@unl.edu

See next page for additional authors

Follow this and additional works at: https://digitalcommons.unl.edu/bioscistorz

Authors

Chandrasekhar Natarajan, Noriko Inoguchi, Roy E. Weber, Angela Fago, Hideaki Moriyama, and Jay F. Storz

Epistasis Among Adaptive Mutations in Deer Mouse Hemoglobin

Chandrasekhar Natarajan,[1] Noriko Inoguchi,[1] Roy E. Weber,[2] Angela Fago,[2] Hideaki Moriyama,[1] and Jay F. Storz [1]

1. School of Biological Sciences, University of Nebraska, Lincoln, NE 68588, USA
2. Zoophysiology, Department of Bioscience, Aarhus University, DK-8000 Aarhus, Denmark
Corresponding author — Jay F. Storz, email jstorz2@unl.edu

Abstract
Epistatic interactions between mutant sites in the same protein can exert a strong influence on pathways of molecular evolution. We performed protein engineering experiments that revealed pervasive epistasis among segregating amino acid variants that contribute to adaptive functional variation in deer mouse hemoglobin (Hb). Amino acid mutations increased or decreased Hb-O_2 affinity depending on the allelic state of other sites. Structural analysis revealed that epistasis for Hb-O_2 affinity and allosteric regulatory control is attributable to indirect interactions between structurally remote sites. The prevalence of sign epistasis for fitness-related biochemical phenotypes has important implications for the evolutionary dynamics of protein polymorphism in natural populations.

Nonadditive interactions between mutations (epistasis) can exert a strong influence on the rate and direction of evolutionary change (1, 2). Insights into mechanisms of epistasis between beneficial mutations can reveal the causes of constraints on adaptive protein evolution (3–10). Mechanisms of epistasis are often best revealed through detailed examinations of interactions between amino acid mutations in the same protein that contribute to variation in a measurable biochemical phenotype (7, 9–15). Such studies are especially relevant to our understanding of evolutionary process when genetically based changes in the measured phenotype contribute to variation in fitness under natural conditions.

We investigated the nature of epistatic interactions between adaptive mutations in the hemoglobin (Hb) of deer mice (*Peromyscus maniculatus*). Deer mice that are native to high altitude have evolved an elevated Hb-O_2 affinity relative to lowland conspecifics (16–18), and this modification of protein function contributes to an adaptive enhancement of whole-animal physiological performance under hypoxia (19, 20). Comparisons between highland deer mice from the Rocky Mountains and lowland deer mice from the Great Plains revealed genetic differences in Hb-O_2 affinity that are attributable to the independent or joint effects of 12 amino acid polymorphisms: 8 mutations in the α-chain subunits of the $\alpha_2\beta_2$ Hb tetramer, and 4 mutations in the β-chain subunits.

These 12 amino acid polymorphisms exhibit pronounced altitudinal shifts in allele frequency, and population genetic analyses of nucleotide variation in the α- and β-globin genes revealed evidence for divergent selection between deer mouse populations that are native to different elevations (18, 21–23).

Structural variation in deer mouse Hb has a modular organization that reflects the linkage arrangement of the 12 amino acid polymorphisms. Within the α-chain subunit, five amino acid replacements are located in exon 2 of the underlying gene, and the remaining three replacements are located in exon 3. Polymorphic sites within the same exon are in nearly complete linkage disequilibrium (LD) with one another, but intragenic recombination has produced a partial uncoupling between the two exons (21, 23). The two most common α-globin allele classes are distinguished from each other by eight amino acid replacements at sites 50, 57, 60, 64, 71, 113, 115, and 116 (Figure S1A). The four amino acid polymorphisms in the β-globin gene are also in nearly complete LD with one another (18, 22). The two most common β-globin allele classes are distinguished from each other by four amino acid replacements at sites 62, 72, 128, and 135 (Figure S1B). Thus, in deer mouse populations, most of the naturally occurring variation in Hb structure is captured by combinatorial permutations of allelic variants at three loci: α-globin exon 2, α-globin exon 3, and β-globin.

We used site-directed mutagenesis to engineer all eight combinations of the α- and β-chain variants in recombinant Hb (rHb), and we measured O_2-binding properties of the purified proteins (24). In addition to the chimeric multipoint mutants, we also engineered 10 additional single- and double-mutant rHbs to measure the functional effects of specific point mutations individually and in pairwise combination. We synthesized rHbs representing the two most common variants from high- and low-altitude populations, designated "HH-H" and "LL-L," respectively (the first two letters denote the separate α-chain subdomains encoded by exons 2 and 3, and the third letter denotes the β-chain subunit). To test for epistasis, we also synthesized rHbs representing the remaining six combinations of H- and L-type alleles at each of the three loci (Figure 1A). To examine variation in the allosteric regulation of Hb-O_2 affinity, we measured O_2-binding properties of each rHb mutant in the presence and absence of the two principal allosteric effectors present in mammalian red blood cells: Cl⁻ ions and 2,3-diphosphoglycerate (DPG). These effectors reduce Hb-O_2 affinity by preferentially binding and stabilizing deoxyHb, thereby shifting the allosteric equilibrium in favor of the low-affinity T-state quaternary structure. By using standardized concentrations of Cl⁻ and DPG in the physiological range, we ensured that in vitro measurements were relevant to in vivo conditions (24).

Our experiments revealed substantial variation in intrinsic Hb-O$_2$ affinity, as P_{50} values (the O$_2$ tension at 50% heme saturation) for stripped, cofactor-free rHbs ranged from 4.55 to 7.09 torr (Table 1). The high-altitude HH-H variant exhibited a 26% lower stripped P_{50} (i.e., higher intrinsic O$_2$ affinity) relative to the low-altitude LL-L variant (Table 1). Hb-O$_2$ affinity was reduced in the presence of Cl$^-$ ions (added as 0.1 M KCl), in the presence of DPG at a twofold molar excess over tetrameric Hb, and in the simultaneous presence of both effectors (Table 1). All rHbs exhibited cooperative O$_2$ binding, and Hill coefficients ranged from 1.36 to 2.28 in the presence of Cl$^-$ and DPG.

Contrary to the expectations of an additive null model, the phenotypic effects of allelic substitutions (L→H and H→L) at α-globin exon 2, α-globin exon 3, and β-globin were highly dependent on ge-netic background, as pairwise epistasis accounted for 40% of the variance in P_{50} values in the absence of allosteric effectors and 90% in the simultaneous presence of Cl$^-$ and DPG (Table 1). In the presence of both allosteric effectors, the HH α-globin allele conferred an increased affinity on the βL background and a decreased affinity on the βH background. Similarly, the H-type β-globin allele conferred an increased affinity on the αLL background and a decreased affinity on the αHH background. These are examples of sign epistasis (2), where the sign of the phenotypic effect of an allele is conditional on genetic background.

Because mammalian Hb is a heterotetramer (α$_2$β$_2$), epistatic interactions could involve closely linked sites in the same gene or sites in unlinked genes that encode different subunits of the protein. Intragenic (within-subunit) epistasis could stem from localized modifications of secondary or tertiary structure, whereas intergenic (between-subunit) epistasis could stem from allosteric transitions in quaternary structure between different oxygenation states of the Hb tetramer. Epistasis for Hb-O$_2$ affinity is mainly attributable to the suppressed DPG sensitivity of chimeric rHb variants that incorporate the products of α- and β-globin alleles of unlike type (αHH combined with βL, and vice versa; Table 1 and Figure 1B). Although DPG sensitivity was suppressed in HH-L and LL-H, allosteric regulatory capacities of the chimeric rHbs were partially restored by reciprocally converting either of the two α-chain subdomains to the type that matched the associated β-chain subunit: DPG sensitivity of the chimeric LL-H was partially restored by L→H substitutions at α-globin exon 2 or exon 3, and reciprocally, DPG sensitivity of the chimeric HH-L was par-
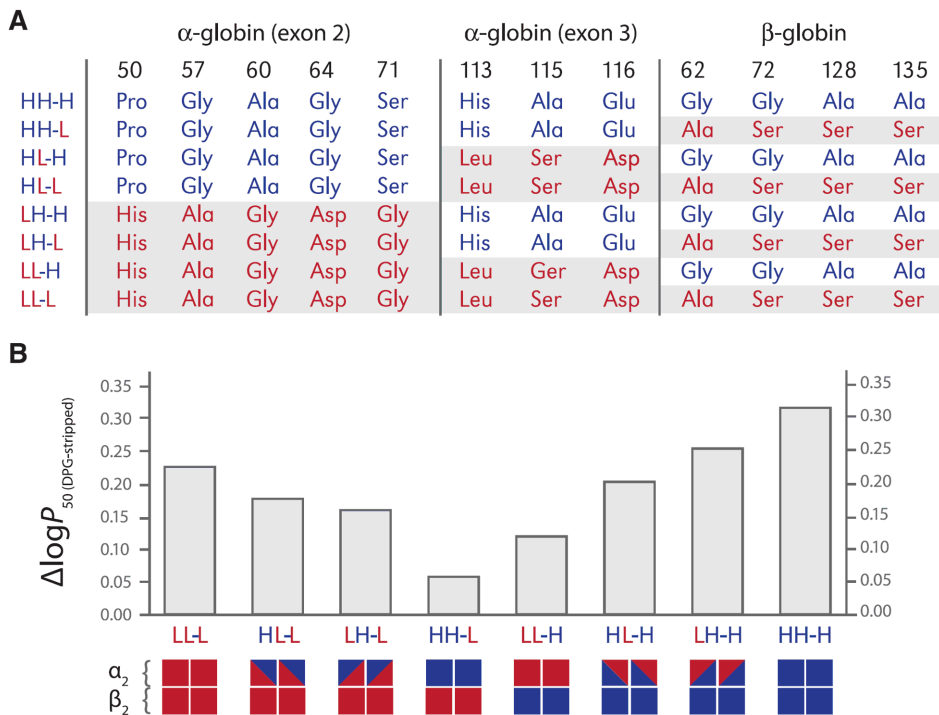

Figure 1. Structural and functional variation among recombinant deer mouse Hbs (rHbs). (**A**) rHbs representing all combinatorial permutations of allelic variants at α-globin exon 2, α-globin exon 3, and β-globin. Shaded regions represent the products of low-altitude L-type alleles (red), and unshaded regions represent products of high-altitude H-type alleles (blue). (**B**) Variation in the allosteric regulation of Hb-O$_2$ affinity by DPG. Sensitivity to DPG is indexed by the difference in log-transformed P_{50} values between stripped Hb in the presence and absence of DPG.

Table 1. O$_2$ affinities (P_{50}, torr; mean ± SEM) and allosteric properties of purified rHbs. Sensitivities to allosteric effectors are measured as the difference in log-transformed P_{50} values in the presence and absence of each effector, individually and in combination. V_A and V_E are estimated components of additive and epistatic variance, respectively (24).

	LL-L	HL-L	LH-L	HH-L	LL-H	HL-H	LH-H	HH-H	V_A	V_E
P_{50} (torr)										
stripped	5.72 ± 0.23	6.37 ± 0.05	7.09 ± 0.55	6.59 ± 0.11	5.25 ± 0.09	5.49 ± 0.04	6.32 ± 0.15	4.55 ± 0.08	0.597	0.403
+KCl	10.20 ± 0.03	12.55 ± 0.41	10.83 ± 0.78	12.88 ± 0.27	12.15 ± 0.31	11.18 ± 0.30	12.01 ± 0.20	9.70 ± 0.47	0.051	0.949
+DPG	9.72 ± 0.17	9.64 ± 0.12	10.33 ± 0.20	7.54 ± 0.25	6.93 ± 0.19	8.84 ± 0.26	11.44 ± 0.30	9.53 ± 0.27	0.189	0.811
+KCl + DPG	10.46 ± 0.30	11.21 ± 0.33	12.51 ± 0.59	8.63 ± 0.21	7.65 ± 0.22	11.36 ± 0.34	12.83 ± 0.34	10.13 ± 0.35	0.096	0.904
$\Delta log\ P_{50}$										
KCl − stripped	0.251	0.295	0.184	0.291	0.364	0.309	0.279	0.329	0.671	0.329
DPG − stripped	0.230	0.180	0.163	0.058	0.121	0.206	0.258	0.321	0.726	0.274
(KCl + DPG) − stripped	0.262	0.246	0.247	0.117	0.164	0.316	0.308	0.348	0.214	0.786

tially restored by H→L substitutions at these same loci (Figure 1B). In principle, a suppressed DPG sensitivity (and hence, increased Hb-O_2 affinity) could be produced by charge-changing amino acid replacements that eliminate phosphate-binding sites in the β-chain subunits. Because the positively charged phosphate-binding sites are invariant in deer mouse β chains (17, 18), allelic variation in DPG sensitivity must stem from indirect, second-order perturbations.

Analysis of the crystal structure of deer mouse Hb at 1.8 Å resolution (24, 25) revealed that each of the eight rHb mutants is characterized by a unique constellation of hydrogen bonds within and between subunits (Table 2 and Figure S2). Additional hydrogen bonds between subunits of the same αβ dimer are formed in the presence of β128Ser (an L-type residue; Figure S2), which contributes to the

observed epistasis between allelic α- and β-chain variants. Structural analysis also revealed that in Hbs with L-type α-globin, the imidazole ring of α50His forms a hydrogen bond with α30Glu in the same subunit. The replacement of α50His with Pro (the H-type residue) eliminates this hydrogen bond and causes a subtle reorientation of the E helix and CD loop (Figure 2), an effect that propagates to the α1β2 intersubunit contact and shifts the allosteric equilibrium in favor of the high-affinity oxyHb (R-state) quaternary structure.

To test the effects of charge-changing α-chain mutations in the CD loop (α50His/Pro) and the adjacent E helix (α64Asp/Gly), we synthesized each of the alternative single and double mutants on both HH-H and LL-L backgrounds. The experiments revealed that, on the LL-L background, substitutions of H-type residues (α50His→Pro and α64Asp→Gly) did not

produce a significant increase in Hb-O_2 affinity individually or in combination; however, on the HH-H background, single-step reversions to L-type residues at both sites produced significant reductions in Hb-O_2 affinity in the presence of allosteric effectors (Figure S3). We also measured the individual effects of all four amino acid mutations in the β-chain subunit. On the LL-L background, the substitution β128Ser→Ala, which removes an α1β1 hydrogen bond (Figure S2), produced an increased anion sensitivity (and hence, a decreased Hb-O_2 affinity in the presence of Cl⁻ and DPG; Figure S4). However, on this same background, introducing all four H-type β-chain mutations in combination produced a highly significant increase in Hb-O_2 affinity in the presence of allosteric effectors (Figure S4).

In summary, results of our mutagenesis experiments revealed pervasive epistasis among segregating amino acid variants in deer mouse Hb (Table 1). The individual and joint effects of α- and β-chain point mutations contribute to the elevated Hb-O_2 affinity of highland deer mice, but the effects of these mutations are highly dependent on the allelic state of other residue positions.

Directed mutagenesis studies have unveiled "cryptic" epistasis between amino acid substitutions that distinguish deeply diverged orthologous proteins (7, 11, 13, 14). Similarly, experimental studies of microbial systems have revealed intragenic epistasis between sites that underwent successive allelic substitutions but that were never simultaneously polymorphic (6, 10). By contrast, the interacting mutations in deer mouse Hb are segregating in natural populations and, given the extensive intragenic and intergenic LD, the epistasis contributes to additive genetic variance in Hb function, providing an explanation for the previously documented variation in anion sensitivity of deer mouse Hbs (17, 18). Given the evidence for spatially varying selection on Hb polymorphism in relation to altitude, the pervasiveness of sign epistasis for Hb-O_2 affinity suggests that the selection coefficient for a given allele will often be highly dependent on the allelic composition of the local population. Thus, sign epistasis among segregating amino acid variants may exert a strong influence on allele frequency dynamics and mutational pathways of protein evolution.

Table 2 Allelic variation in the network of atomic contacts within and between subunits of deer mouse Hb. Plus signs denote the presence of hydrogen bonds within subunits (α50His-α30Glu and α113His-α24Tyr) or between subunits of unlike type (α34Cys-β128Ser). Polymorphic sites are shown in bold.

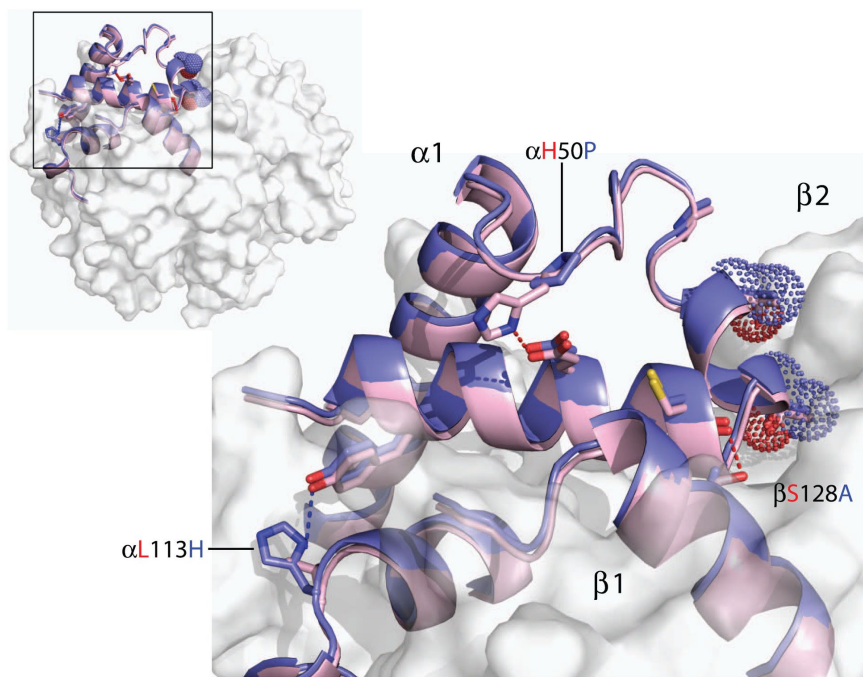|	LL-L	HL-L	LH-L	HH-L	LL-H	HL-H	LH-H	HH-H
H-bonds								
α50His-α30Glu	+			+		+		+
α113His-α24Tyr			+	+			+	+
α34Cys-**β128Ser**	+	+	+	+				

Figure 2. Difference in the network of hydrogen bonds between high- and low-altitude Hb variants, HH-H and LL-L, respectively. The α1 and β1 subunits of HH-H (light blue) and LL-L (light red) are superimposed, and van der Waals radii are shown for α-chain residues that are in atomic contact with β-chain residues of the opposing α2β2 dimer.

Supplementary Materials appear following References and Notes.

Materials and Methods
Figs. S1 to S5
Table S1
References (26–41)

References and Notes

1. F. J. Poelwijk, D. J. Kiviet, D. M. Weinreich, S. J. Tans, *Nature* 445, 383 (2007).
2. D. M. Weinreich, R. A. Watson, L. Chao, *Evolution* 59, 1165 (2005).
3. J. da Silva, M. Coetzer, R. Nedellec, C. Pastore, D. E. Mosier, *Genetics* 185, 293 (2010).
4. M. A. DePristo, D. M. Weinreich, D. L. Hartl, *Nat. Rev. Genet.* 6, 678 (2005).
5. D. J. Kvitek, G. Sherlock, *PLoS Genet.* 7, e1002056 (2011).
6. E. R. Lozovsky *et al.*, *Proc. Natl. Acad. Sci. U.S.A.* 106, 12025 (2009).
7. M. Lunzer, S. P. Miller, R. Felsheim, A. M. Dean, *Science* 310, 499 (2005).
8. D. R. Rokyta *et al.*, *PLoS Genet.* 7, e1002075 (2011).
9. M. L. Salverda *et al.*, *PLoS Genet.* 7, e1001321 (2011).
10. D. M. Weinreich, N. F. Delaney, M. A. Depristo, D. L. Hartl, *Science* 312, 111 (2006).
11. J. T. Bridgham, E. A. Ortlund, J. W. Thornton, *Nature* 461, 515 (2009).
12. B. Lehner, *Trends Genet.* 27, 323 (2011).
13. M. Lunzer, G. B. Golding, A. M. Dean, *PLoS Genet.* 6, e1001162 (2010).
14. E. A. Ortlund, J. T. Bridgham, M. R. Redinbo, J. W. Thornton, *Science* 317, 1544 (2007).
15. P. C. Phillips, *Nat. Rev. Genet.* 9, 855 (2008).
16. J. F. Storz, *J. Mammal.* 88, 24 (2007).
17. J. F. Storz, A. M. Runck, H. Moriyama, R. E. Weber, A. Fago, *J. Exp. Biol.* 213, 2565 (2010).
18. J. F. Storz *et al.*, *Proc. Natl. Acad. Sci. U.S.A.* 106, 14450 (2009).
19. M. A. Chappell, J. P. Hayes, L. R. G. Snyder, *Evolution* 42, 681 (1988).
20. M. A. Chappell, L. R. G. Snyder, *Proc. Natl. Acad. Sci. U.S.A.* 81, 5484 (1984).
21. J. F. Storz, J. K. Kelly, *Genetics* 180, 367 (2008).
22. J. F. Storz, C. Natarajan, Z. A. Cheviron, F. G. Hoffmann, J. K. Kelly, *Genetics* 190, 203 (2012).
23. J. F. Storz *et al.*, *PLoS Genet.* 3, e45 (2007).
24. Materials and methods are attached following the References.
25. N. Inoguchi *et al.*, *Acta Crystallogr. Sect. F Struct. Biol. Cryst. Commun.* 69, 393 (2013).

Supplementary Materials for

Epistasis Among Adaptive Mutations in Deer Mouse Hemoglobin

Chandrasekhar Natarajan, Noriko Inoguchi, Roy E. Weber, Angela Fago, Hideaki Moriyama, Jay F. Storz*

*Corresponding author. E-mail: jstorz2@unl.edu

This PDF file includes:

Materials and Methods

Vector construction. Nucleotide sequences of deer mouse globin genes were optimized with respect to *E. coli* codon preferences, and were then synthesized by GenScript (Piscataway, NJ, USA). Gene cassettes for the α- and β-globin genes and the *methionine aminopeptidase* (*MAP*) gene were tandemly cloned into the custom expression vector described by Natarajan *et al*. (*26*). In order to maximize efficiency in the post-translational cleaving of N-terminal methionines from the α- and β-chain polypeptides, an additional copy of the *MAP* gene was cloned into the pCO-MAP plasmid with a kanamycin resistance gene and was co-expressed with the pGM expression plasmid.

Mutagenesis. Using the HH-H and LL-L pGM plasmid vector templates, cassette mutagenesis was performed by switching out HH- and L-type sequences of α- and β-globin genes, thereby yielding the chimeric HH-L and LL-H constructs. To synthesize the remaining constructs, the same plasmids were used as templates for site-directed mutagenesis using the QuikChange® II XL Site-Directed Mutagenesis kit from Stratagene (LaJolla, CA, USA). In each plasmid construct, engineered codon changes were verified by DNA sequencing. Sequences for the mutagenic primers are provided in Table S1 and sequences of the synthesized α- and β-globin genes are provided in Fig. S5.

Expression and purification of recombinant hemoglobin. All rHbs were expressed in *E. coli* JM109 (DE3). The bacterial cells were subject to dual selection in an LB agar plate containing ampicillin and kanamycin. This double selection ensures that transformed cells receive both the pGM and pCO-MAP plasmids. Large-scale production was conducted in batches containing 1-1.5 L of TB medium. Cells were grown at 37ºC in an orbital shaker at 200 rpm until the absorbance reached 0.6-0.8 at 600 nm. Expression of the Hb and MAP genes was induced with 0.2 mM IPTG and the cell culture was supplemented with hemin (50 µg/ml) and glucose (20 g/L). The cells were then grown at 28ºC for 16 hr in an orbital shaker at 200 rpm. The bacterial culture was saturated with CO for 15 min and the cells were harvested by centrifugation. Recombinant Hbs were purified by means of HPLC as described previously (*26*). To confirm that the absorbance maxima of the purified rHb samples matched those of native Hbs, we measured absorbance spectra of oxy, deoxy, and CO derivatives at 450-600 nm.

O$_2$ equilibrium experiments. O$_2$-binding equilibria of rHb solutions (0.2 mM heme) were measured at 37ºC in 0.1 M Hepes buffer, pH 7.4, in the absence (stripped) and presence of added effectors (0.1 M KCl, and/or DPG at 2.0-fold molar excess over rHb tetramers). These are standard experimental conditions (*27, 28*) that closely approximate *in vivo* effector concentrations: 100 mM Cl$^-$ approximates the naturally occurring concentration inside mammalian red blood cells (where K$^+$ is the main counter ion, as opposed to Na$^+$ in the plasma) and a DPG/Hb tetramer ratio = 2.0 falls within the physiological range for deer mice and most other eutherian mammals (*28-35*). Moreover, standardized measurements of purified Hb are essential for assessing the potentially subtle effects of individual amino acid mutations and for making meaningful comparisons of Hb-O$_2$ affinity across studies (*27, 28, 36*).

Measurements on purified Hb solutions in the presence and absence of Cl$^-$ and DPG at physiological levels provide insights into mechanisms of allosteric regulation by revealing whether measured differences in Hb function are attributable to differences in intrinsic O_2-affinity and/or differences in sensitivity to anionic effectors (*27, 28, 37*). The rHb concentration used in our O_2-equilibrium experiments (0.2 mM heme) is also standard (*27, 28*).

Measures of Hb-O_2 affinity were conducted using a modified diffusion chamber where changes in absorbance are recorded during stepwise changes in the O_2 tension of equilibration gases (*36*). Each O_2-equilibrium curve was based on 4-6 saturation steps. Values of P_{50} (O_2 tension at half-saturation) and the cooperativity coefficient, n_{50}, were obtained from the zero-intercept and the slope of Hill plots, respectively: $(\log(Y/(1-Y))$ vs. $\log PO_2$, where Y is the fractional O_2 saturation. Standard errors of the measured P_{50} values were calculated by using nonlinear regression to fit the O_2-binding data to the Hill equation. Measured P_{50} values for the isolated rHbs were consistent with those for native Hbs from high- and low-altitude deer mice under identical experimental conditions (*17-18*).

Measuring epistasis. For the set of eight multi-point rHb mutants, we used a regression model to measure the additive and epistatic components of variance in P_{50} and $\Delta\log$-P_{50} values: $y = \mu + \beta_1 x_1 + \beta_2 x_2 + \beta_3 x_3 + \beta_{12} x_1 x_2 + \beta_{13} x_1 x_3 + \beta_{23} x_2 x_3 +$ error, where coefficients for x_1, x_2, and x_3 measure the main effects of allelic variants at the three discrete globin modules (α-globin exon 2, α-globin exon 3, and β-globin), and coefficients for $x_1 x_2$, $x_1 x_3$, and $x_2 x_3$ measure each of the three possible pairwise interaction effects.

To measure pairwise epistasis for Hb-O_2 affinity between a given pair of mutant sites, we measured the epistatic deviation (ε) from the expectations of an additive model: $\varepsilon = (P_{ii} + P_{jj}) - (P_{ij} + P_{ji})$, where P_{ij} is the measured P_{50} of the rHb that incorporates the products of alleles i and j at each of two sites. The standard error of the measured epistatic deviation, a linear function of P_{ij}, was calculated using the method of error propagation $\sigma_\varepsilon = \sqrt{\sigma P_{ii}^2 + \sigma P_{jj}^2 + \sigma P_{ij}^2 + \sigma P_{ji}^2}$, and the 95% confidence interval for ε was computed as $\varepsilon \pm \sigma_\varepsilon \times 1.96$. Epistasis between a given pair of mutant sites was considered to be statistically significant if the 95% confidence interval for ε did not include zero.

Structural analysis. To elucidate the structural mechanisms that are responsible for the additive and epistatic effects of the various α- and β-chain mutations on Hb-O_2 affinity, we used the crystal structure of the LL-L rHb (PDB ID, 4h2l) to build a structural model for HH-H using MODELLER 9V11 (*38*) and SWISS-MODEL (*39*). Human Hb structures (2dn1, 2dn2, and 2dn3) (*40*) were used as controls. Molecular interactions were identified by PISA (*41*), and molecular graphics were generated using PyMol (Schrödinger, LLC).

(A) α-chain variants	50	57	60	64	71	113	115	116
α^{I}	Pro	Gly	Ala	Gly	Ser	His	Ala	Glu
α^{II}	His	Gly	Ala	Gly	Ser	His	Ala	Glu
α^{III}	Pro	Gly	Ala	Gly	Ser	His	Ala	Asp
α^{IV}	His	Gly	Ala	Gly	Ser	His	Ala	Asp
α^{V}	Pro	Gly	Ala	Gly	Ser	Leu	Ser	Asp
α^{VI}	His	Gly	Ala	Asp	Gly	Leu	Ser	Asp
α^{VII}	His	Ala	Gly	Asp	Gly	Leu	Ser	Asp

(B) β-chain variants	62	72	128	135
β^{I}	Gly	Gly	Ala	Ala
β^{II}	Ala	Gly	Ala	Ala
β^{III}	Ala	Ser	Ser	Ser

Fig. S1. Amino acid combinations that define the most common α- and β-chain Hb variants in highland and lowland deer mice. (A) Seven allelic α-globin variants defined by different 8-site amino acid combinations. The α^{I} sequence represents the most common α-chain variant in highland mice, and the α^{VII} sequence represents the most common variant in lowland mice. (B) Three allelic β-globin variants defined by different 4-site amino acid combinations. The β^{I} sequence represents the most common β-chain variant in highland mice, and the β^{III} sequence represents the most common variant in lowland mice. Characteristic H- and L-type allelic variants are shown in blue and red, respectively.

A) HH-H (α113H-α24Y)   B) LL-L (α50H-α30E, β128S-α34C)

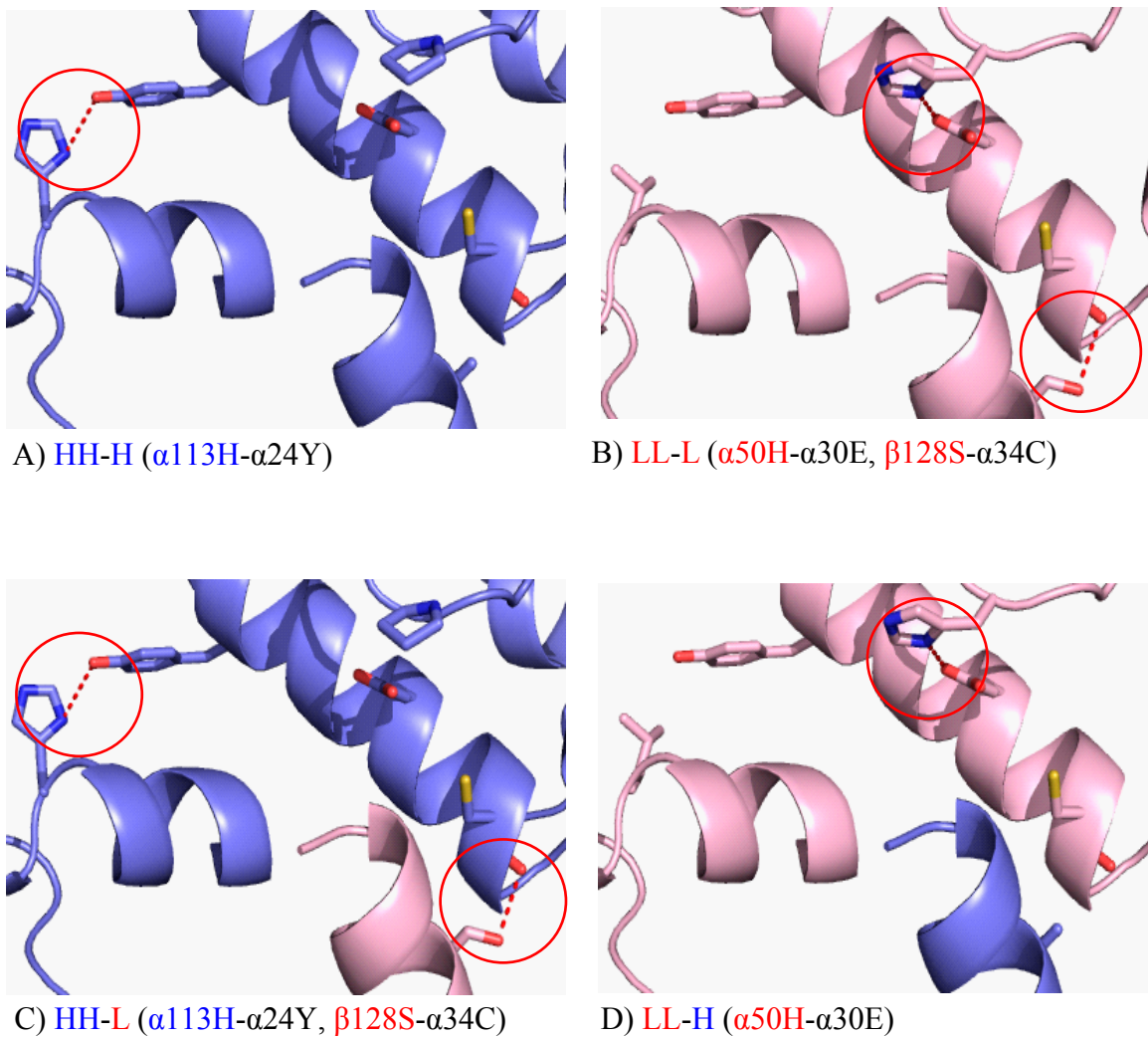C) HH-L (α113H-α24Y, β128S-α34C)   D) LL-H (α50H-α30E)

Fig. S2. Presence and absence of hydrogen-bonds in the two most common high- and low-altitude Hb variants (HH-H and LL-L, respectively) and hybrid tetramers (HH-L and LL-H). The α50His-α30Glu bond (depicted in B and D) and the α113His-α24Tyr bond (depicted in A and C) represent points of contact between α-helices or interhelical loops within the same α-chain subunit. The α34Cys-β128Ser bond (depicted in B and C) represents an intradimer (α1β1 and α2β2) contact. For each polymorphic amino acid site, the alpha-numerical designation for each variant residue is shown in blue or red depending on whether it represents a high-altitude (H-type) or low-altitude (L-type) variant, respectively.
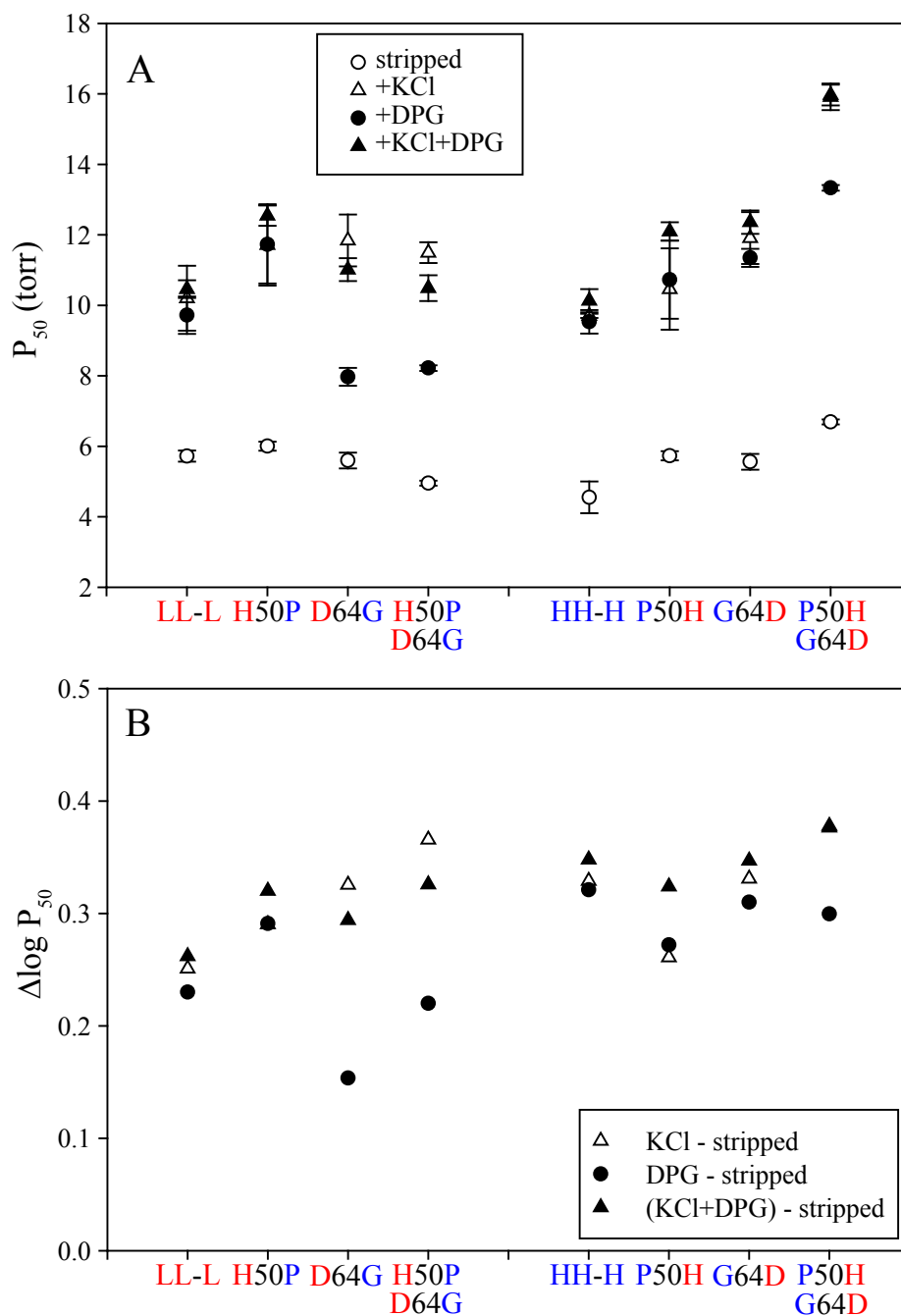
Fig. S3. Individual and pairwise effects of charge-changing α-chain mutations on alternative genetic backgrounds. In forward mutagenesis experiments using the LL-L background, H-type mutations were introduced individually (H50P and D64G) and in combination (H50P/D64G). In reverse mutagenesis experiments using the HH-H background, both sites were reverted to L-type residues individually (P50H and G64D) and in combination (P50H/G64D). (A) Variation in P_{50} values in the presence and absence of allosteric effectors (Cl⁻ and DPG). Error bars represent 95% confidence intervals. (B) Variation in the sensitivity to allosteric effectors, as indexed by the log-transformed difference in P_{50} values in the presence and absence of each effector individually and in combination (see text for details).
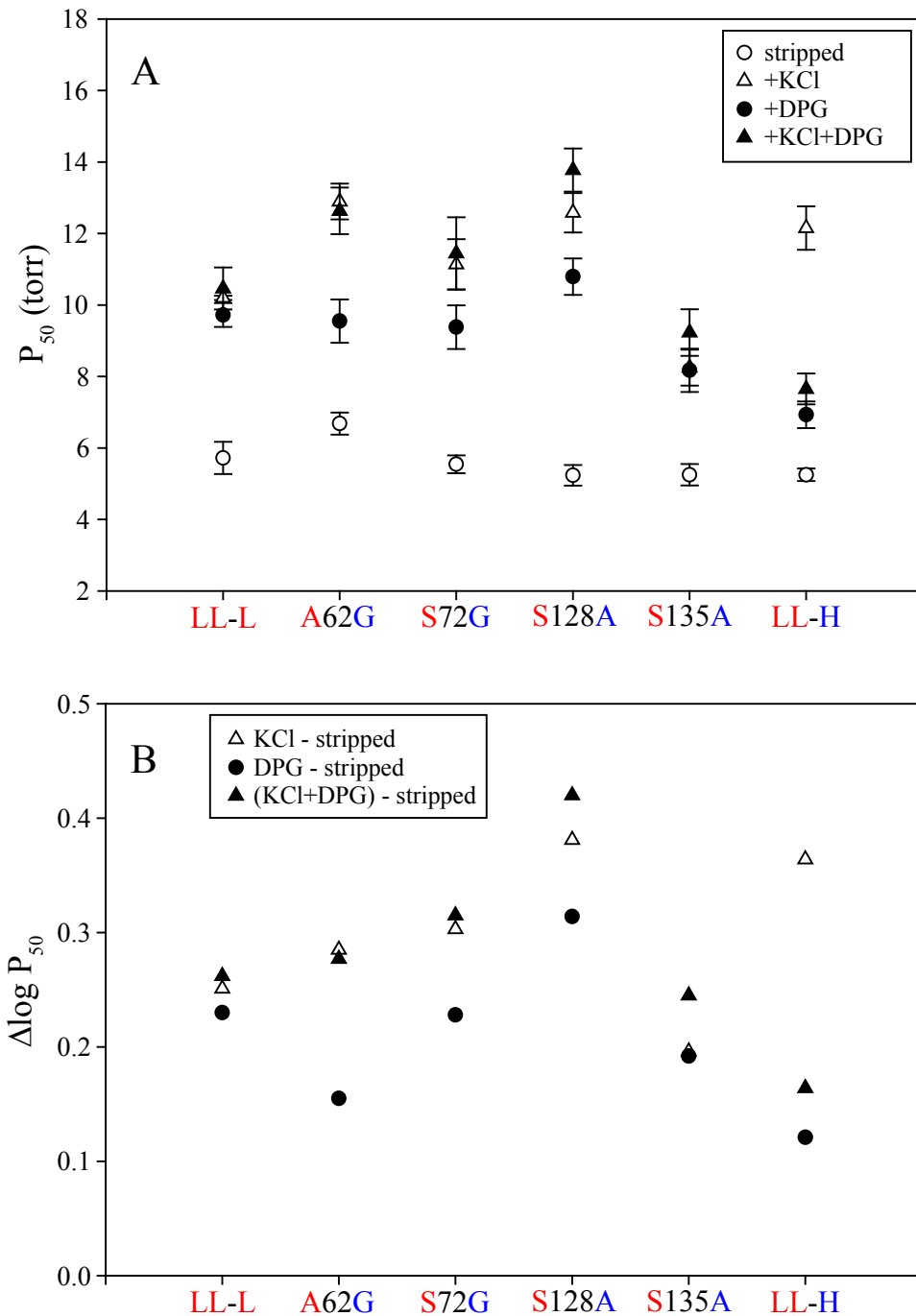
Fig. S4. Individual and combined effects of β-globin point mutations on the LL-L background. Comparison between 'LL-L' and 'LL-H' reveals the net effect of all four β-chain mutations in combination. (A) Variation in P_{50} values in the presence and absence of allosteric effectors (Cl^- and DPG). Error bars represent 95% confidence intervals. (B) Variation in the sensitivity to allosteric effectors, as indexed by the log-transformed difference in P_{50} values in the presence and absence of each effector individually and in combination (see text for details).

A) α-globin

```
        1         10        20        30        40        50        60        70
αHH  VLSADDKAN IK AAWGK IGGHG AEYGAE ALER  MFCS FP TTK TYF PH F DVS PGS AQVK GHG AKV AGALATAAS HLDD
αHL  VLSADDKAN IK AAWGK IGGHG AEYGAE ALER  MFCS FP TTK TYF PH F DVS PGS AQVK GHG AKV AGALATAAS HLDD
αLH  VLSADDKAN IK AAWGK IGGHG AEYGAE ALER  MFCS FP TTK TYF PH F DVS HGS AQVK AHG GKV ADALATAAG HLDD
αLL  VLSADDKAN IK AAWGK IGGHG AEYGAE ALER  MFCS FP TTK TYF PH F DVS HGS AQVK AHG GKV ADALATAAG HLDD

        80        90        100       110       120       130       141
αHH  LPAALSALS DLHAHK LRVDPVN FK   LLSHCLLV TLAAH H PAEF TPAVHAS LDK FLASVS TVLTSK YR
αHL  LPAALSALS DLHAHK LRVDPVN FK   LLSHCLLV TLAAH LPS DF TPAVHAS LDK FLASVS TVLTSK YR
αLH  LPAALSALS DLHAHK LRVDPVN FK   LLSHCLLV TLAAH H PAEF TPAVHAS LDK FLASVS TVLTSK YR
αLL  LPAALSALS DLHAHK LRVDPVN FK   LLSHCLLV TLAAH LPS DF TPAVHAS LDK FLASVS TVLTSK YR
```

B) β-globin

```
        1         10        20        30        40        50        60        70
βH   VH LTDAEK ALV TG LWGKVK PEE IGGEALG  R LLAVY PWTQR FFDS FG DLSS ASA IMGN AKVK GHGKKV IDS FG EGL
βL   VH LTDAEK ALV TG LWGKVK PEE IGGEALG  R LLAVY PWTQR FFDS FG DLSS ASA IMGN AKVK AHGKKV IDS FS EGL

        80        90        100       110       120       130       140       146
βH   KH LDN LKG TFAS LS ELH CDK LHV DPEN FK  LLGNMIV IVMAHH LGK DFTPAAQ AA YQKVV AGVATALAHK YH
βL   KH LDN LKG TFAS LS ELH CDK LHV DPEN FK  LLGNMIV IVMAHH LGK DFTPAAQ S AYQKVV SGVATALAHK YH
```

Fig. S5. Amino acid sequences of globin alleles that were incorporated in recombinant deer mouse Hbs. The sequences represent (A) the four alternative α-globin variants (HH, HL, LH, and LL) and (B) the two alternative β-globin variants (H and L). H- and L-type residues at variable sites are shown in blue and red, respectively. Spaces in each sequence alignment separate regions that are encoded by exons 1-3.

8

Table S1. Sequences of PCR primers used for site-directed mutagenesis.

Name	Primer sequence
LLA62G_SEN	atcatgggtaacgctaaagttaaaggtcacggtaaaaaagttatc
LLA62G_ANTI	gataactttttaccgtgacctttaactttagcgttacccatgat
LLS72G_SEN	taaaaaagttatcgactctttcggtgaaggtctgaaacacctggac
LLS72G_ANTI	gtccaggtgtttcagaccttcaccgaaagagtcgataacttttta
LLS128A_SEN	ccccggctgctcaggctgcttaccagaaag
LLS128A_ANTI	ctttctggtaagcagcctgagcagccgggg
LLS135A_SEN	agtctgcttaccagaaagttgttgctggtgttgctac
LLS135A_ANTI	gtagcaacaccagcaacaactttctggtaagcagact
LSD_SEN	ctggctgctcacctcccgagtgatttcaccccggctg
LSD_ ANTI	cagccggggtgaaatcactcgggaggtgagcagccag
HAE_ SEN	ctggctgctcaccatccggctgagttcaccccggctg
HAE_ ANTI	cagccggggtgaactcagccggatggtgagcagccag
HHP50H_SEN	ccgcacttcgacgtttctcatggttctgctcaggttaaag
HHP50H_ANTI	ctttaacctgagcagaaccatgagaaacgtcgaagtgcgg
HHG65D_SEN	gtgctaaagttgctgatgctctggctaccgc
HHG65D_ANTI	gcggtagccagagcatcagcaactttagcac
LLH50P_SEN	cacttcgacgtttctcccggttctgctcaggtt
LLH50P_ANTI	aacctgagcagaaccgggagaaacgtcgaagtg
LLD64G_SEN	gtggtaaagttgctggcgctctggctaccgc
LLD64G_ANTI	gcggtagccagagcgccagcaactttaccac

References and Notes

1. F. J. Poelwijk, D. J. Kiviet, D. M. Weinreich, S. J. Tans, Empirical fitness landscapes reveal accessible evolutionary paths. *Nature* **445**, 383–386 (2007). doi:10.1038/nature05451 Medline

2. D. M. Weinreich, R. A. Watson, L. Chao, Perspective: Sign epistasis and genetic constraint on evolutionary trajectories. *Evolution* **59**, 1165–1174 (2005). Medline

3. J. da Silva, M. Coetzer, R. Nedellec, C. Pastore, D. E. Mosier, Fitness epistasis and constraints on adaptation in a human immunodeficiency virus type 1 protein region. *Genetics* **185**, 293–303 (2010). doi:10.1534/genetics.109.112458 Medline

4. M. A. DePristo, D. M. Weinreich, D. L. Hartl, Missense meanderings in sequence space: A biophysical view of protein evolution. *Nat. Rev. Genet.* **6**, 678–687 (2005). [doi:10.1038/nrg1672](doi:10.1038/nrg1672) Medline

5. D. J. Kvitek, G. Sherlock, Reciprocal sign epistasis between frequently experimentally evolved adaptive mutations causes a rugged fitness landscape. *PLoS Genet.* **7**, e1002056 (2011). doi:10.1371/journal.pgen.1002056 Medline

6. E. R. Lozovsky, T. Chookajorn, K. M. Brown, M. Imwong, P. J. Shaw, S. Kamchonwongpaisan, D. E. Neafsey, D. M. Weinreich, D. L. Hartl, Stepwise acquisition of pyrimethamine resistance in the malaria parasite. *Proc. Natl. Acad. Sci. U.S.A.* **106**, 12025–12030 (2009). doi:10.1073/pnas.0905922106 Medline

7. M. Lunzer, S. P. Miller, R. Felsheim, A. M. Dean, The biochemical architecture of an ancient adaptive landscape. *Science* **310**, 499–501 (2005). doi:10.1126/science.1115649 Medline

8. D. R. Rokyta, P. Joyce, S. B. Caudle, C. Miller, C. J. Beisel, H. A. Wichman, Epistasis between beneficial mutations and the phenotype-to-fitness Map for a ssDNA virus. *PLoS Genet.* **7**, e1002075 (2011). doi:10.1371/journal.pgen.1002075 Medline

9. M. L. Salverda, E. Dellus, F. A. Gorter, A. J. Debets, J. van der Oost, R. F. Hoekstra, D. S. Tawfik, J. A. de Visser, Initial mutations direct alternative pathways of protein evolution. *PLoS Genet.* **7**, e1001321 (2011). doi:10.1371/journal.pgen.1001321 Medline

10. D. M. Weinreich, N. F. Delaney, M. A. Depristo, D. L. Hartl, Darwinian evolution can follow only very few mutational paths to fitter proteins. *Science* **312**, 111–114 (2006). doi:10.1126/science.1123539 Medline

11. J. T. Bridgham, E. A. Ortlund, J. W. Thornton, An epistatic ratchet constrains the direction of glucocorticoid receptor evolution. *Nature* **461**, 515–519 (2009). doi:10.1038/nature08249 Medline

12. B. Lehner, Molecular mechanisms of epistasis within and between genes. *Trends Genet.* **27**, 323–331 (2011). [doi:10.1016/j.tig.2011.05.007](doi:10.1016/j.tig.2011.05.007) Medline

13. M. Lunzer, G. B. Golding, A. M. Dean, Pervasive cryptic epistasis in molecular evolution. *PLoS Genet.* **6**, e1001162 (2010). doi:10.1371/journal.pgen.1001162 Medline

14. E. A. Ortlund, J. T. Bridgham, M. R. Redinbo, J. W. Thornton, Crystal structure of an ancient protein: Evolution by conformational epistasis. *Science* **317**, 1544–1548 (2007). doi:10.1126/science.1142819 Medline

15. P. C. Phillips, Epistasis—the essential role of gene interactions in the structure and evolution of genetic systems. *Nat. Rev. Genet.* **9**, 855–867 (2008). [doi:10.1038/nrg2452](doi:10.1038/nrg2452) Medline

16. J. F. Storz, Hemoglobin function and physiological adaptation to hypoxia in high-altitude mammals. *J. Mammal.* **88**, 24–31 (2007). doi:10.1644/06-MAMM-S-199R1.1

17. J. F. Storz, A. M. Runck, H. Moriyama, R. E. Weber, A. Fago, Genetic differences in hemoglobin function between highland and lowland deer mice. *J. Exp. Biol.* **213**, 2565–2574 (2010). [doi:10.1242/jeb.042598](doi:10.1242/jeb.042598) Medline

18. J. F. Storz, A. M. Runck, S. J. Sabatino, J. K. Kelly, N. Ferrand, H. Moriyama, R. E. Weber, A. Fago, Evolutionary and functional insights into the mechanism underlying high-altitude adaptation of deer mouse hemoglobin. *Proc. Natl. Acad. Sci. U.S.A.* **106**, 14450–14455 (2009). doi:10.1073/pnas.0905224106 Medline

19. M. A. Chappell, J. P. Hayes, L. R. G. Snyder, Hemoglobin polymorphisms in deer mice (*Peromyscus maniculatus*): Physiology of beta-globin variants and alpha-globin recombinants. *Evolution* **42**, 681 (1988). [doi:10.2307/2408859](doi:10.2307/2408859)

20. M. A. Chappell, L. R. G. Snyder, Biochemical and physiological correlates of deer mouse alpha-chain hemoglobin polymorphisms. *Proc. Natl. Acad. Sci. U.S.A.* **81**, 5484–5488 (1984). doi:10.1073/pnas.81.17.5484 Medline

21. J. F. Storz, J. K. Kelly, Effects of spatially varying selection on nucleotide diversity and linkage disequilibrium: Insights from deer mouse globin genes. *Genetics* **180**, 367–379 (2008). doi:10.1534/genetics.108.088732 Medline

22. J. F. Storz, C. Natarajan, Z. A. Cheviron, F. G. Hoffmann, J. K. Kelly, Altitudinal variation at duplicated β-globin genes in deer mice: Effects of selection, recombination, and gene conversion. *Genetics* **190**, 203–216 (2012). doi:10.1534/genetics.111.134494 Medline

23. J. F. Storz, S. J. Sabatino, F. G. Hoffmann, E. J. Gering, H. Moriyama, N. Ferrand, B. Monteiro, M. W. Nachman, The molecular basis of high-altitude adaptation in deer mice. *PLoS Genet.* **3**, e45 (2007). doi:10.1371/journal.pgen.0030045 Medline

24. Materials and methods are available as supplementary materials on *Science* Online.

25. N. Inoguchi, J. R. Oshlo, C. Natarajan, R. E. Weber, A. Fago, J. F. Storz, H. Moriyama, Deer mouse hemoglobin exhibits a lowered oxygen affinity owing to mobility of the E helix. *Acta Crystallogr. Sect. F Struct. Biol. Cryst. Commun.* **69**, 393–398 (2013). [doi:10.1107/S1744309113005708](doi:10.1107/S1744309113005708) Medline

26. C. Natarajan, X. Jiang, A. Fago, R. E. Weber, H. Moriyama, J. F. Storz, Expression and purification of recombinant hemoglobin in *Escherichia coli*. *PLoS ONE* **6**, e20176 (2011). doi:10.1371/journal.pone.0020176 Medline

27. K. Imai, *Allosteric Effects in Hemoglobin* (Cambridge Univ. Press, Cambridge, UK, 1982).

28. H. Mairbäurl, R. E. Weber, *Compr. Physiol.* **2**, 1463 (2011). doi:10.1002/cphy.c080113

29. R. Baumann, C. Bauer, H. Bartels, Influence of chronic and acute hypoxia on oxygen affinity and red cell 2,3 diphosphoglycerate of rats and guinea pigs. *Respir. Physiol.* **11**, 135–144 (1971). [doi:10.1016/0034-5687(71)90018-1](doi:10.1016/0034-5687(71)90018-1) Medline

30. H. F. Bunn, Differences in the interaction of 2,3-diphosphoglycerate with certain mammalian hemoglobins. *Science* **172**, 1049–1050 (1971). doi:10.1126/science.172.3987.1049 Medline

31. J. Duhm, Effects of 2,3-diphosphoglycerate and other organic phosphate compounds on oxygen affinity and intracellular pH of human erythrocytes. *Pflugers Arch.* **326**, 341–356 (1971). doi:10.1007/BF00586998 Medline

32. J. Duhm, E. Gerlach, On the mechanisms of the hypoxia-induced increase of 2,3-diphosphoglycerate in erythrocytes. *Pflugers Arch.* **326**, 254–269 (1971). doi:10.1007/BF00592506 Medline

33. H. Mairbäurl, O. Oelz, P. Bärtsch, Interactions between Hb, Mg, DPG, ATP, and Cl determine the change in Hb-O_2 affinity at high altitude. *J. Appl. Physiol.* **74**, 40–48 (1993). Medline

34. L. R. G. Snyder, 2,3-diphosphoglycerate in high- and low-altitude populations of the deer mouse. *Respir. Physiol.* **48**, 107–123 (1982). doi:10.1016/0034-5687(82)90053-6 Medline

35. D. M. Tufts, I. G. Revsbech, Z. A. Cheviron, R. E. Weber, A. Fago, J. F. Storz, Phenotypic plasticity in blood-oxygen transport in highland and lowland deer mice. *J. Exp. Biol.* **216**, 1167–1173 (2013). doi:10.1242/jeb.079848 Medline

36. R. E. Weber, Use of ionic and zwitterionic (Tris/BisTris and HEPES) buffers in studies on hemoglobin function. *J. Appl. Physiol.* **72**, 1611–1615 (1992). Medline

37. M. F. Perutz, Mechanisms of cooperativity and allosteric regulation in proteins. *Q. Rev. Biophys.* **22**, 139–237 (1989). doi:10.1017/S0033583500003826 Medline

38. A. Šali, T. L. Blundell, Comparative protein modelling by satisfaction of spatial restraints. *J. Mol. Biol.* **234**, 779–815 (1993). doi:10.1006/jmbi.1993.1626 Medline

39. K. Arnold, L. Bordoli, J. Kopp, T. Schwede, The SWISS-MODEL workspace: A web-based environment for protein structure homology modelling. *Bioinformatics* **22**, 195–201 (2006). doi:10.1093/bioinformatics/bti770 Medline

40. S. Y. Park, T. Yokoyama, N. Shibayama, Y. Shiro, J. R. Tame, 1.25 A resolution crystal structures of human haemoglobin in the oxy, deoxy and carbonmonoxy forms. *J. Mol. Biol.* **360**, 690–701 (2006). doi:10.1016/j.jmb.2006.05.036 Medline

41. E. Krissinel, K. Henrick, Inference of macromolecular assemblies from crystalline state. *J. Mol. Biol.* **372**, 774–797 (2007). doi:10.1016/j.jmb.2007.05.022 Medline